ARTICLE

Engineering the Microstructure of Organic Energetic Materials

Gengxin Zhang, Huizhong Sun, Jason M. Abbott, and Brandon L. Weeks*

Chemical Engineering, Texas Tech University, Lubbock, Texas 79409

ABSTRACT The initiation sensitivity is highly dependent on void structures within an energetic material. It is technically feasible to modify the initiation sensitivity by lithographically defining the size and distribution of included voids on the micro- and nanoscale. We proposed a method to pattern organic energetic materials using microcontact printing of self-assembled monolayers. Pentaerythritol tetranitrate is spin-coated from solution as films onto patterned self-assembled monolayers. Images are presented for arbitrary patterns created based on the surface chemistry and concentration of the energetic material.

KEYWORDS: atomic force microscopy • energetic materials • explosives • PETN • initiation • microcontact printing

INTRODUCTION

The sensitivity and reaction propagation rate of explosives depend strongly on the particle size distribution, surface area, and void volume within the energetic material. The effect of voids on the impact initiation was recognized by Apin and Bobolev (1) in the 1940s. In order to incorporate voids, explosive materials are typically formulated such that the theoretical maximum density is in the range of 50−95% and is controlled by the packing and particle size of the explosive (2). Even though it is widely recognized that included voids modify the sensitivity and/or output of explosives for ignition and propagation, universal agreement is lacking about the optimum size of the voids or the mechanism that leads to ignition (3).

One mechanism of initiation suggests that the voids contribute to detonation by creating "hot spots" (4) as the shock wave propagates through the material. The "hot spots" result when voids undergo a strong shock, resulting in adiabatic compression, and heating, to several thousands of degrees (5). Once formed, these hot spots may fail to react chemically because of thermal diffusion, or they may react exothermically, thus creating an ignition site in the solid explosive. These ignition sites then grow in temperature, size, and pressure, leading to a deflagration or detonation depending on the physical and chemical properties of the material. This mechanism has not received universal acceptance, however. Other studies have concluded that compression of the voids depends upon the strength of the initiation stimulus and that shear or plastic work effects may better explain ignition (6−8).

The sensitivity of explosives is also highly influenced by the void size. Mechanically damaged explosives, for example, can be more sensitive because of an increase in the number, and size, of voids (9, 10). There is no universal agreement on the optimum void size, but it is generally assumed to be in the range of ~100 nm to a few micrometers (11, 12). Outside this range, when the void is too large, its collapse leads to a deflagration of the explosive either because of dissipative energy loss mechanisms or by a reduced volume fraction of the energetic material. On the other hand, if the void is too small, its collapse will not yield a high enough temperature to propagate the reaction (3, 13). By far, the majority of research investigating the effect of the void size on initiation and propagation is computational (14, 15). Experimental work, directly incorporating voids, has typically relied on using microspheres of a specific size where the spatial distribution of the microspheres is not controlled (16). To date, there have been limited efforts to control the size, shape, and period of the void structure within an organic energetic material.

Continuous films of explosives have been prepared by a number of methods including spin coating and thermal evaporation (17). Although large areas (cm) with thicknesses greater than 1 μm could be created using these methods, voids were not lithographically defined. Other methods of modifying energetic materials on the micro- and nanoscale have used probe microscopy. King et al. (18) were able to show that thin-film energetic materials can be modified by using a heated microcantilever to sublime or decompose the energetic material locally, and Nafday et al. (19) performed dip-pen nanolithography to directly deposit energetic materials with nanometer precision. However, neither of the scanning probe methods is suitable for large-scale production of voids in energetic materials.

It is technically feasible to design and construct highly complicated ordered structures of energetic materials to control the ignition and propagation of the explosive. One option is to change the substrate surface energy such that explosives deposited will self-assemble based on the underlying chemistry. Dlott (20) initially proposed creating ordered arrays of metallic energetic materials by using self-assembled monolayers (SAMs) to direct the assembly based on hydrophilic/hydrophobic interactions. However, there

* E-mail: Brandon.weeks@ttu.edu.
Received for review January 23, 2009 and accepted April 6, 2009

DOI: 10.1021/am900052k

Published on Web 04/28/2009

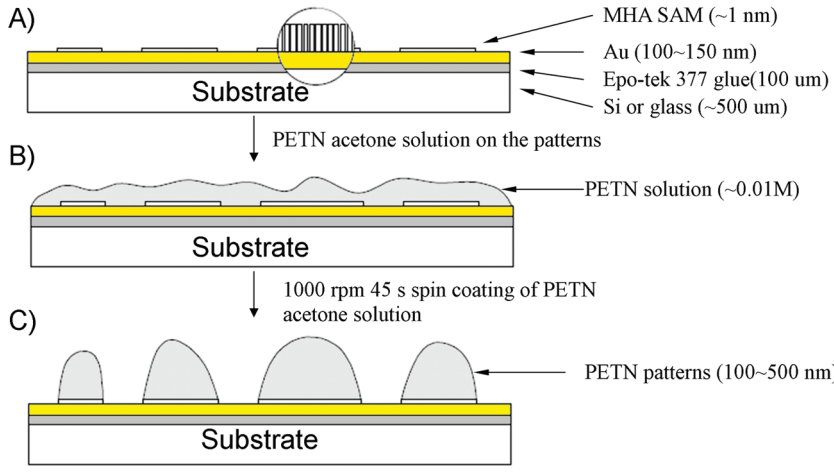

FIGURE 1. Schematic diagram of the experimental procedure (not to scale): (A) A template-stripped gold substrate was coated with an MHA SAM by μ-CP. (B) The substrate was covered with a 0.01 M PETN acetone solution. (C) The PETN pattern formed on the substrate areas stamped with MHA after spin coating.

were no attempts to create patterns of organic energetic materials in that review.

One method of changing the surface chemistry of a substrate is to use alkanethiol SAMs on gold, where the terminal chemistry of the SAM defines the surface energy (21, 22). In addition, SAM patterns can easily be lithographically defined through microcontact printing (μ-CP) (21). During the printing process, a SAM pattern, with defined features, is transferred from a stamp to a wide range of substrates. By using μ-CP, specific areas of the substrate can have different surface energies and can thus be selectively wetted. After the patterns are generated, another material, which has an affinity to one of the patterned areas, is subsequently deposited. This generic approach has been used to achieve thin-film transistors composed of conductive and semiconductive polymers (23, 24).

In the case of subsequent deposition of a material on a surface, the fabrication of patterns is governed by growth phenomena that are typically nonequilibrium processes (25–27). Growth is ultimately governed by the competition between the kinetics of deposition and the thermodynamics of the interaction between the substrate and the deposited molecule (28). For example, if the surface diffusion rate of the deposited molecules is slower compared to the pattern formation rate, the pattern growth is essentially determined by the kinetics and leads to stable structures (27). Therefore, kinetic control provides an elegant way to manipulate the structure and morphology of surfaces. Here, we present a method of creating patterns of pentaerythritol tetranitrate (PETN) deposited on alkanethiol SAMs.

EXPERIMENTAL SECTION

Materials. Absolute ethanol (99.99%, Sigma-Aldrich Inc., St. Louis, MO) was used as the solvent and cleaning agent in the experiment. Three alkanethiols (all purchased from Sigma-Aldrich Inc.), 11-mercapto-1-undecanol [$HS(CH_2)_{11}OH$, 99%; MUO], 16-mercaptohexadecanoic acid [$HS(CH_2)_{15}CO_2H$, 97%; MHA], and 1-undcanethiol [$CH_3(CH_2)_{10}SH$, 98%], were used in our experiment. These three alkanethiols were chosen to provide a variety of substrate surface energies ranging from hydrophilic to hydrophobic. PETN [obtained from Lawrence Livermore National Laboratory (LLNL), Livermore, CA, with purity of 99%] solutions were prepared using acetone as the solvent with concentrations ranging from 0.1 to 0.001 M.

Preparation of Gold Substrates. Gold films were prepared with template stripping gold reported by Wagner et al. (29). A thermal evaporator operating at 10^{-6}–10^{-7} Torr was used to deposit 100–200 nm of gold (99.99%) onto cleaved mica (Allied Electronics Inc., Fort Worth, TX). The mica was cleaned, prior to coating, in a solution containing 9 parts H_2O_2 (30% solution) and 1 part NH_4OH (20%) (30) and rinsed with deionized water. Polished silicon wafers (Nova Electronic Materials Ltd., Flower Mound, TX) were diced into 1 cm × 1 cm pieces and treated with a Piranha etch solution (98% H_2SO_4 and 30% H_2O_2 in volume ratios of 3:1; ***Caution!*** *this solution is strongly acidic and corrosive*) under agitation for 30 min and then rinsed with deionized water. The cleaned silicon pieces were glued onto the gold side of the coated mica using Epo-Tek 377 (Epoxy Technology Inc., Billerica, NM) and annealed at 100–150 °C for 2 h. The substrates were stored in a vacuum desiccator before use. Prior to use, the silicon was peeled from the mica, leaving a fresh gold surface for μ-CP.

μ-CP. Poly(dimethylsiloxane) (PDMS) stamps were provided by LLNL. Each alkanethiol was dissolved in ethanol to make a 10 mM solution. The solution was added dropwise to the PDMS stamp until completely covered in the solution. The stamp was allowed to dry in air prior to use. Details of the printing process and fabrication methods used to prepare stamps are described elsewhere (22, 31).

PETN Pattern Formation. PETN films were formed by dropwise application of the solution to the stamped substrate and spin coating at 1000 rpm for 45 s. A schematic of the overall process used is shown in Figure 1.

Contact Angles. Water contact angle measurements (using a Ramé-Hart model-100 goniometer equipped with a CCD camera) were obtained for each type of monolayer with the sessile drop technique at room temperature and constant humidity. The drop snake method (32) was used to determine the contact angle of each type of monolayer by analyzing the images collected by the CCD camera. Water contact angles on MHA, MUO, 1-undecanthiol SAMs, and PETN crystal are 32.0 ± 3°, 45.1 ± 3°, 108.0 ± 3°, and 64.0 ± 3°, respectively.

Imaging. Surface morphology was characterized with a NanoScope IIIa multimode atomic force microscope (Veeco Instruments, Santa Barbara, CA) operating in tapping mode. All imaging was performed at scan rates of 0.60 Hz using a cantilever drive frequency of ~325 kHz. A standard optical

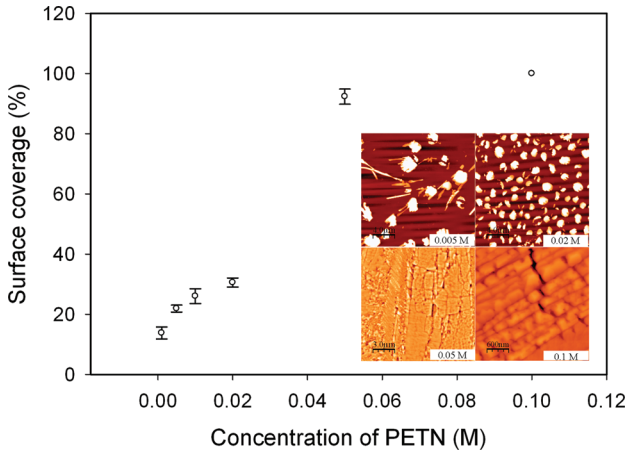

FIGURE 2. Surface coverage changes with the concentration of PETN. Insets: AFM tapping mode topographic images of the corresponding concentrations.

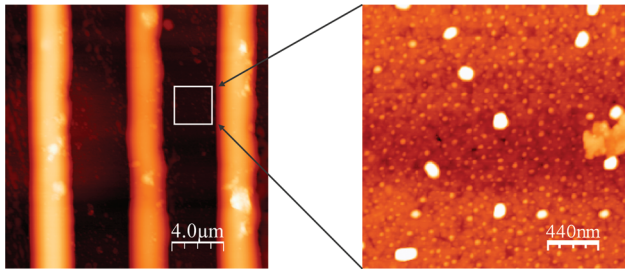

FIGURE 3. AFM image of PETN lines patterned on an MHA SAM surface (20 × 20 μm^2). Inset: High-magnification image of the native gold (2.2 × 2.2 μm^2).

microscope (AmScope Inc., Chino, CA) was used to collect the optical image of the patterns.

RESULTS AND DISCUSSION

The PETN films formed on the alkanethiol SAMs appear to follow the Yong−Dupre principle (33) and are proposed to be most dependent on the surface energy. However, it cannot be ruled out that there is a chemical interaction between the acid group on the SAM and the nitroether group on the PETN. Our results suggest that interaction between the PETN molecules and substrates can be adjusted by the surface energy with different thiol SAMs. A number of thiols were investigated to form thin films including MUO, MHA, and 1-undecanthiol. These three alkanethiols were chosen based on their different surface energies (water contact angles given in the experimental section). Although it was possible to create films on both MUO and 1-undecanthiol, it was difficult to achieve reproducible, continuous films, even at high concentrations. Using the most hydrophilic surface, MHA, continuous PETN films could easily be generated.

Initial experiments were conducted to determine the optimal concentration of PETN required in making reproducible surfaces with complete coverage on MHA. These surfaces were not stamped but rather the SAM was formed by soaking the gold in the thiol solution for 30 min. Figure 2 shows the results on surface coverage based on the PETN concentration and corresponding atomic force microscopy (AFM) images. At lower concentrations, disconnected layers form on the substrate. Above ~0.05 M PETN, a continuous layer is formed on the substrate.

Lithography experiments were initially performed by stamping arbitrary patterns of MHA onto a gold surface. Then PETN was coated by spin-casting as described above. AFM images of the lines are shown in Figure 3. During the spin-casting, the PETN solution is deposited over the entire surface (both stamped and unstamped regions). It is proposed that during drying PETN migrates to the MHA patterned surface. This has been shown to be the case with other materials deposited in a similar fashion (34, 35). High-resolution AFM images were also collected in the unstamped region for comparison to the coated regions. Calculations

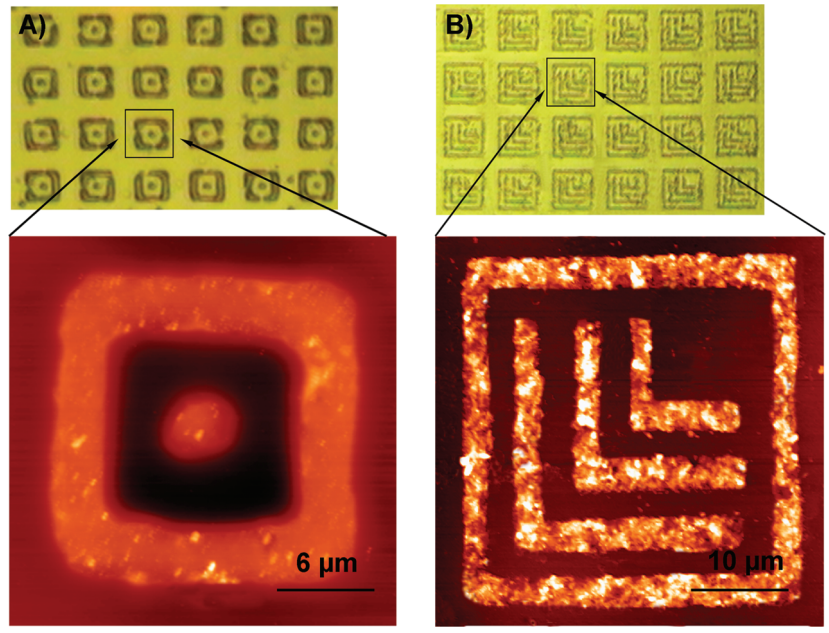

FIGURE 4. Optical images of PETN formation on the complex patterns. Scale bars are as shown in the pictures. Tapping-mode AFM image of complex patterns on the MHA SAM surface. Scan area: (A) 30 × 30 μm^2; (B) 50 × 50 μm^2.

comparing the volume of PETN in the MHA-coated and -uncoated regions indicate that the uncoated region had less than 3% of total coverage (~0.01% by total mass).

In order to use this method in creating structures for initiation studies in energetic materials, we demonstrated its general applicability by using it to create arbitrary patterns. We prepared a complex square and a "triple L" pattern prepared with the same procedure. Optical images and AFM images are shown in Figure 4. Although the optical images appear to show that the films are not continuous, the AFM images demonstrate that continuous coating is achieved. It is believed that optical effects based on the localized thickness, density, and/or crystallinity in the nanometer thin film give rise to differences in the optical images.

Although other methods can be used to deposit PETN on surfaces, patterning of PETN on gold surfaces has been shown to be difficult using thermal evaporation to make continuous films on gold because the rapid nucleation of PETN often results in dendrites or faceted crystals (36). In addition, thermal evaporation may decompose the explosive during deposition. Hence, the pattering method proposed in this study is a unique approach, where with control of the concentration and substrate surface energy, continuous films and arbitrary patterns of explosives can be generated.

CONCLUSION

μ-CP of SAMs in combination with subsequent deposition can potentially be used as a universal patterning approach for energetic materials. By careful control of the pattern size, shape, and period, this technique can provide a new method for studying the mechanisms of initiation and propagation in energetic materials where inhomogeneity has been shown to be an important parameter (4). Thus far, there have been no techniques to produce well-ordered arrays of high explosives where both the voids and the energetic component can be controlled. The procedure outlined can be used to produce patterns with vertical and lateral dimensions ranging from 100 nm up to many micrometers and may lead to a better understanding of the initiation mechanisms based on "hot spot" formation.

Acknowledgment. The authors acknowledge support received from NSF CAREER-JA (CBET-0644832) and DHS ALERT-HS and ONR-GZ (N00014-06-1-0922). The authors thank Alex Noy (LLNL) for the PDMS stamps and Susan Barrick (Texas Tech University) for helpful discussions. This material is based upon work supported by the U.S. Department of Homeland Security under Award No. 2008-ST-061-ED0001. The views and conclusions contained in this document are those of the authors and should not be interpreted as necessarily representing the official policies, either expressed or implied, of the U.S. Department of Homeland Security.

REFERENCES AND NOTES

(1) Apin, A. Y.; Bobolev, V. K. *Zh. Fiz. Khim.* **1946**, *20*, 1367–1370.
(2) Edmonds, E.; Hazelwood, A.; Lilly, T.; Mansell, J. *Powder Technol.* **2007**, *174*, 42–45.
(3) Howe, P. M. *Prog. Astronaut. Aeronaut.* **2000**, *185*, 141–183.
(4) Field, J. E.; Bourne, N. K.; Palmer, S. J. P.; Walley, S. M. *Philos. Trans. R. Soc. London, Ser. A* **1992**, *339*, 269–283.
(5) Bourne, N. K.; Milne, A. M. *Proc. R. Soc. London, A* **2003**, *459*, 1851–1861.
(6) Baker, P. J.; Mellor, A. M. *Combust. Sci. Technol. Book Ser.* **1997**, *4*, 289–316.
(7) Shi, Y. F.; Brenner, D. W. In *Symposium on Theory, Modeling and Numerical Simulation of Multi-Physics Materials Behavior Held at the 2007 MRS Fall Meeting*; Tikare, V., Murch, G. E., Soisson, F., Kang, J. K., Eds.; Trans Tech Publications Ltd.: Boston, MA, 2007; pp 77–82.
(8) Mellor, A. M.; Wiegand, D. A.; Isom, K. B. *Combust. Flame* **1995**, *101*, 26–35.
(9) Menikoff, R. In *Meeting of the Health Communication Division of the Western-States-Communication-Association*; Furnish, M. D., Gupta, Y. M., Forbes, J. W., Eds.; American Institute of Physics: Long Beach, CA, 2002; pp 393–396.
(10) Chen, P. W.; Huang, F. L.; Ding, Y. S. *Prog. Saf. Sci. Technol., Vol. III, Parts A and B* **2002**, *3*, 1417–1422.
(11) Maienschein, J. L.; Urtiew, P. A.; Garcia, F.; Chandler, J. B. *AIP Conf. Proc.* **1998**, *429*, 711–714.
(12) Hirosaki, Y.; Murata, K.; Kato, Y.; Itoh, S. *AIP Conf. Proc.* **2002**, *620*, 930–933.
(13) Bourne, N. K.; Field, J. E. *Proc. Math. Phys. Eng. Sci.* **1999**, *455*, 2411–2426.
(14) Yano, K.; Horie, Y.; Greening, D. *Impact Eng. Appl., Proc. Int. Symp., Vols. I and II* **2001**, 201–206.
(15) Willey, T. M.; van Buuren, T.; Lee, J. R. I.; Overturf, G. E.; Kinney, J. H.; Handly, J.; Weeks, B. L.; Ilavsky, J. *Propellants, Explos., Pyrotech.* **2006**, *31*, 466–471.
(16) Hamate, Y. *Shock Compression Condens. Matter, Parts 1 and 2* **2007**, *955*, 923–926.
(17) Ericson, K. L.; Skocypec, R. D.; Trott, W. M.; Renlund, A. M. *Proceedings of the 15th International Pyrotechnics Seminar*; IIT Research Institute: Chicago, IL, 1990; p 199.
(18) King, W. P.; Saxena, S.; Nelson, B. A.; Weeks, B. L.; Pitchimani, R. *Nano Lett.* **2006**, *6*, 2145–2149.
(19) Nafday, O. A.; Pitchimani, R.; Weeks, B. L.; Haaheim, J. *Propellants, Explos., Pyrotech.* **2006**, *31*, 376–381.
(20) Dlott, D. D. *Mater. Sci. Technol.* **2006**, *22*, 463–473.
(21) Kumar, A.; Whitesides, G. M. *Appl. Phys. Lett.* **1993**, *63*, 2002–2004.
(22) Kumar, A.; Biebuyck, H. A.; Whitesides, G. M. *Langmuir* **1994**, *10*, 1498–1511.
(23) Liang, C. H.; Chen, L. C.; Hwang, J. S.; Chen, K. H.; Hung, Y. T.; Chen, Y. F. *Appl. Phys. Lett.* **2002**, *81*, 22–24.
(24) Sirringhaus, H.; Kawase, T.; Friend, R. H.; Shimoda, T.; Inbasekaran, M.; Wu, W.; Woo, E. P. *Science* **2000**, *290*, 2123–2126.
(25) Casimirius, S.; Flahaut, E.; Laberty-Robert, C.; Malaquin, L.; Carcenac, F.; Laurent, C.; Vieu, C. *Microelectron. Eng.* **2004**, *73–74*, 564–569.
(26) Roder, H.; Hahn, E.; Brune, H.; Bucher, J. P.; Kern, K. *Nature* **1993**, *366*, 141–143.
(27) Braun, H.-G.; Meyer, E.; Wang, M. *Lect. Notes Phys.* **2003**, *606*, 238–251.
(28) Erhardt, M. K.; Nuzzo, R. G. *J. Phys. Chem. B* **2001**, *105*, 8776–8784.
(29) Wagner, P.; Hegner, M.; Guentherodt, H.-J.; Semenza, G. *Langmuir* **1995**, *11*, 3867–3875.
(30) Kim, D.; Pitchimani, R.; Snow David, E.; Hope-Weeks Louisa, J. *Scanning* **2008**, *30*, 118–122.
(31) Xia, Y.; Whitesides, G. M. *Angew. Chem., Int. Ed.* **1998**, *37*, 550–575.
(32) Stalder, A. F.; Kulik, G.; Sage, D.; Barbieri, L.; Hoffmann, P. *Colloids Surf., A* **2006**, *286*, 92–103.
(33) Lupis, C. H. P. *Chemical Thermodynamics of Materials*; Elsevier: New York, 1983.
(34) Tuccitto, N.; Giamblanco, N.; Licciardello, A.; Marletta, G. *Chem. Commun.* **2007**, 2621–2623.
(35) Briseno, A. L.; Aizenberg, J.; Han, Y.-J.; Penkala, R. A.; Moon, H.; Lovinger, A. J.; Kloc, C.; Bao, Z. *J. Am. Chem. Soc.* **2005**, *127*, 12164–12165.
(36) Zhang, G.; Weeks, B. L. *Scanning* **2008**, *30*, 228–231.

AM900052K